FACTA UNIVERSITATIS
Series: **Mechanical Engineering** Vol. 22, Nº 3, Special Issue, 2024, pp. 529 - 545
https://doi.org/10.22190/FUME240322020W

Original scientific paper

SLIDING FRICTION IN CONTACTS WITH ONE- AND TWO-DIMENSIONAL VISCOELASTIC FOUNDATIONS AND VISCOELASTIC HALF-SPACE

Toshiki Watanabe[1], Shintaro Hatanaka[1], Ken Nakano[2], Valentin L. Popov[3]

[1]Graduate School of Environment and Information Sciences,
Yokohama National University, Yokohama, Japan
[2]Faculty of Environment and Information Sciences,
Yokohama National University, Yokohama, Japan
[3]Department of System Dynamics and Friction Physics,
Technische Universität Berlin, Berlin, Germany

ORCID iDs: Toshiki Watanabe https://orcid.org/0009-0006-4442-3074
Shintaro Hatanaka https://orcid.org/0009-0006-4989-6065
Ken Nakano https://orcid.org/0000-0001-7437-7984
Valentin L. Popov https://orcid.org/0000-0003-0506-3804

Abstract. *Solid viscoelasticity is one of the essential origins of sliding friction, as every solid exhibits energy dissipation due to it during deformation processes. In this paper, we first show theoretical solutions for one-dimensional (1D) problems of viscoelastic friction with a 1D viscoelastic foundation. Then, we extend the 1D model to a two-dimensional (2D) model to find theoretical solutions for 2D problems of viscoelastic friction. Finally, we apply the Method of Dimensionality Reduction (MDR) to the theoretical solutions for the 1D problems to discuss three-dimensional (3D) problems of viscoelastic friction.*

Key words: *Sliding friction, Viscoelastic foundations, Viscoelastic half-space, MDR*

1. INTRODUCTION

Solid viscoelasticity is one of the essential origins of sliding friction, as every solid exhibits energy dissipation due to it during deformation processes [1,2]. In theoretical investigation, a viscoelastic foundation consisting of independent rheological elements can be considered an asymptotic model of contacts of a rigid probe with a very thin, compressible viscoelastic layer [3-5]. Another limiting case is a very thick layer, namely the viscoelastic half-space [6-9]. Real systems are in between these two limits.

Received: April 03, 2024 / Accepted May 09, 2024
Corresponding author: Valentin L. Popov
Technische Universität Berlin, Strasse des 17 Juni 135, 10623 Berlin, Germany
E-mail: v.popov@tu-berlin.de

Contact mechanics of viscoelastic foundations is simple [10]. By capitalizing on their simplicity, we can obtain a rough but clear picture of the basics of sliding friction due to solid viscoelasticity [11-14]. For example, we need only five system parameters to describe the sliding contacts of a rigid probe with a Kelvin-Voigt viscoelastic foundation [15]. This simplicity brings master curves for the velocity dependences of several quantities (e.g., the contact width, indentation depth or normal load, friction force, and friction coefficient) described by reasonable dimensionless numbers, showing the effects of the inlet slope and vertical lift on the friction coefficient [16]. This analytical method has been extended to the standard linear solid viscoelasticity, showing how mechanical and material origins for bell-shaped velocity-dependent friction compete [17].

Contact mechanics of half-spaces is much more complicated compared with elastic foundations due to non-locality of elastic and viscoelastic interactions. However, for axisymmetric *normal* contacts, there exist a transformation reducing a three-dimensional (3D) contact into a contact with a one-dimensional (1D) viscoelastic foundation. This transformation is given by the so-called Method of Dimensionality Reduction (MDR) [18]. For normal contact, the MDR provides the exact solution of the initial 3D contact problem [18]. There exists no exact procedure for applying MDR to sliding contacts. However, there are reasons to believe that a formal application of MDR to sliding systems gives qualitatively correct results. Since the famous work by Grosch [19], it is widely accepted that the energy dissipation in rubber friction is mostly due to internal dissipation in the viscoelastic material. Based on this idea and foregoing works [20], Persson suggested in 1998 a simple idea of estimating energy dissipation during sliding [21]. He used the Hertzian solution and assumed that it is realized dynamically with the frequency corresponding to the time of contact of "asperities". This means that he suggested considering the sliding contact as a "repeated normal contact", which surely is not the exact picture of what happens in sliding but a very good qualitative presentation. This idea was used in a later paper by Persson and Tosatti [22] for treating more complicated topographies. This basic idea by Persson means approximate reduction of sliding contact problem to the normal contact problem. However, the normal contact problem is mapped exactly to a problem with a 1D foundation via MDR. This means, the sliding MDR solution will have the same accuracy as the initial concept by Persson. This hypothesis was checked by Kürschner [23] by comparing the formal sliding MDR-solution with the complete 3D Boundary Element Method (BEM) simulations. For contact with a simple fluid, he has shown that the MDR solution and the "numerically exact" solution differ only by a constant factor (depending on the probe shape). Kusche [24] could confirm a very good coincidence of MDR-solution with complete 3D BEM simulation for a number of more complicated rheology. These results show that the MDR procedure can also be used to sliding contacts with elastomers after correcting them by a constant factor of the order unity.

In this paper, we first show theoretical solutions for 1D problems of viscoelastic friction with a 1D viscoelastic foundation (Section 2). Then, we extend the 1D model to a two-dimensional (2D) model to find theoretical solutions for 2D problems of viscoelastic friction (Section 3). Finally, we apply the MDR to the theoretical solutions for the 1D problems to discuss 3D problems of viscoelastic friction (Section 4).

2. Sliding Contacts of Rigid Probes with a 1D Viscoelastic Foundation

2.1. Model for 1D Problems

In Section 2, we consider simple 1D problems. Fig. 1 shows the analytical models for sliding contact between a rigid probe and a 1D viscoelastic foundation. We consider triangular and parabolic probes:

$$h(x) = \tan\theta|x|, \tag{1}$$

$$h(x) = \frac{x^2}{2R}, \tag{2}$$

respectively, where θ is the slope angle of the triangular probe, and R is the tip curvature radius of the parabolic probe. The viscoelastic foundation is a 1D array of independent Kelvin-Voigt elements along the x-axis, characterized by a stiffness (per unit area) K and a damping coefficient (per unit area) C. The indentation depth is δ, and the drive speed of the foundation is V. In this situation, the normal load (per unit length) W' and friction force (per unit length) F' are [16]:

$$W' = \int_{-a}^{b} \left(K(\delta - h) - CV\frac{\mathrm{d}h}{\mathrm{d}x} \right) \mathrm{d}x, \tag{3}$$

$$F' = \int_{-a}^{b} -\frac{\mathrm{d}h}{\mathrm{d}x}\left(K(\delta - h) - CV\frac{\mathrm{d}h}{\mathrm{d}x} \right) \mathrm{d}x, \tag{4}$$

respectively, where a and b represent the positions of the leading and trailing edges of the sliding contact, respectively. The leading edge is determined geometrically, while the trailing edge is determined dynamically (see Eq. (6)). The friction coefficient is obtained by $\mu = F'/W'$.

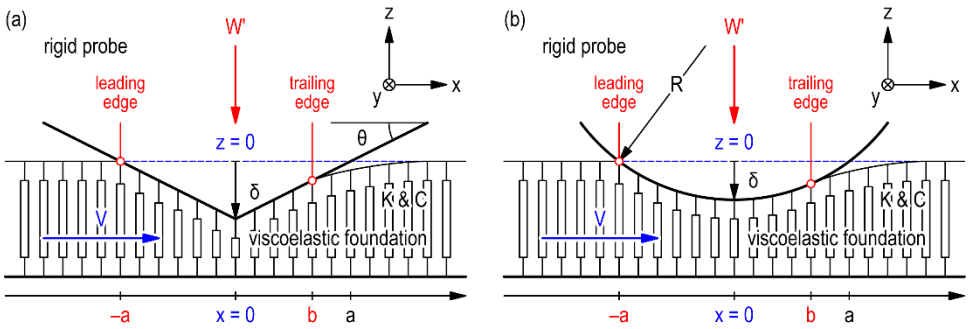

Fig. 1 Analytical models for sliding contact between a rigid probe and a 1D viscoelastic foundation; (a) triangular and (b) parabolic probes.

2.2 Theoretical Solutions for 1D Problems

2.2.1. *Triangular Probe*

In this section, we show the theoretical solutions for the 1D sliding problem of the triangular probe. First, under constant-δ conditions (where the indentation depth is controlled to be constant), the dimensionless drive speed is [16]:

$$\tilde{V}_\delta \equiv \frac{CV\tan\theta}{K\delta}. \tag{5}$$

Then, the normalized outlet contact width, dimensionless normal load, dimensionless friction force, and normalized friction coefficient under constant-δ conditions are given as the following explicit functions of the dimensionless drive speed [16]:

$$\beta \equiv \frac{b}{a} = \begin{cases} 1-\tilde{V}_\delta & \text{for} \quad 0 \le \tilde{V}_\delta \le 1 \\ 0 & \text{for} \quad 1 \le \tilde{V}_\delta \end{cases}, \tag{6}$$

$$\tilde{W}_\delta \equiv \frac{W'\tan\theta}{K\delta^2} = \begin{cases} 1+\frac{1}{2}\tilde{V}_\delta{}^2 & \text{for} \quad 0 \le \tilde{V}_\delta \le 1 \\ \frac{1}{2}+\tilde{V}_\delta & \text{for} \quad 1 \le \tilde{V}_\delta \end{cases}, \tag{7}$$

$$\tilde{F}_\delta \equiv \frac{F'}{K\delta^2} = \begin{cases} 2\tilde{V}_\delta - \frac{1}{2}\tilde{V}_\delta{}^2 & \text{for} \quad 0 \le \tilde{V}_\delta \le 1 \\ \frac{1}{2}+\tilde{V}_\delta & \text{for} \quad 1 \le \tilde{V}_\delta \end{cases}, \tag{8}$$

$$\tilde{\mu}_\delta \equiv \frac{\mu}{\tan\theta} = \begin{cases} \frac{4\tilde{V}_\delta - \tilde{V}_\delta{}^2}{2+\tilde{V}_\delta{}^2} & \text{for} \quad 0 \le \tilde{V}_\delta \le 1 \\ 1 & \text{for} \quad 1 \le \tilde{V}_\delta \end{cases}. \tag{9}$$

Then, under constant-W conditions (where the normal load is controlled to be constant), based on the relationship between δ and W' given by Eq. (7), we obtain the following dimensionless drive speed [16]:

$$\tilde{V}_W \equiv \frac{CV}{K}\left(\frac{K\tan\theta}{W'}\right)^{1/2} = \begin{cases} \tilde{V}_\delta\left(1+\frac{1}{2}\tilde{V}_\delta{}^2\right)^{-1/2} & \text{for} \quad 0 \le \tilde{V}_\delta \le 1 \\ \tilde{V}_\delta\left(\frac{1}{2}+\tilde{V}_\delta\right)^{-1/2} & \text{for} \quad 1 \le \tilde{V}_\delta \end{cases}. \tag{10}$$

From Eq. (10), we obtain the dimensionless drive speed for constant-δ conditions as an explicit function of that for constant-W conditions [16]:

$$\tilde{V}_\delta = \begin{cases} \tilde{V}_W \sqrt{\dfrac{2}{2-\tilde{V}_W{}^2}} & \text{for} \quad 0 \le \tilde{V}_W \le \sqrt{\dfrac{2}{3}} \\ \dfrac{1}{2}\tilde{V}_W{}^2 + \dfrac{1}{2}\tilde{V}_W \sqrt{2+\tilde{V}_W{}^2} & \text{for} \quad \sqrt{\dfrac{2}{3}} \le \tilde{V}_W \end{cases}. \tag{11}$$

Therefore, we obtain the following explicit forms for the other dimensionless quantities under constant-W conditions [16]:

$$\beta \equiv \frac{b}{a} = \begin{cases} 1-\tilde{V}_W \sqrt{\dfrac{2}{2-\tilde{V}_W{}^2}} & \text{for} \quad 0 \le \tilde{V}_W \le \sqrt{\dfrac{2}{3}} \\ 0 \quad \text{for} \quad \sqrt{\dfrac{2}{3}} \le \tilde{V}_W \end{cases}, \tag{12}$$

$$\tilde{\delta}_W \equiv \delta \left(\frac{K}{W' \tan\theta} \right)^{1/2} = \begin{cases} \sqrt{1-\dfrac{1}{2}\tilde{V}_W{}^2} & \text{for} \quad 0 \le \tilde{V}_W \le \sqrt{\dfrac{2}{3}} \\ \sqrt{2+\tilde{V}_W{}^2} - \tilde{V}_W & \text{for} \quad \sqrt{\dfrac{2}{3}} \le \tilde{V}_W \end{cases}, \tag{13}$$

$$\tilde{F}_W \equiv \frac{F'}{W' \tan\theta} = \begin{cases} \tilde{V}_W \sqrt{4-2\tilde{V}_W{}^2} - \dfrac{1}{2}\tilde{V}_W{}^2 & \text{for} \quad 0 \le \tilde{V}_W \le \sqrt{\dfrac{2}{3}} \\ 1 \quad \text{for} \quad \sqrt{\dfrac{2}{3}} \le \tilde{V}_W \end{cases}, \tag{14}$$

$$\tilde{\mu}_W \equiv \frac{\mu}{\tan\theta} = \begin{cases} \tilde{V}_W \sqrt{4-2\tilde{V}_W{}^2} - \dfrac{1}{2}\tilde{V}_W{}^2 & \text{for} \quad 0 \le \tilde{V}_W \le \sqrt{\dfrac{2}{3}} \\ 1 \quad \text{for} \quad \sqrt{\dfrac{2}{3}} \le \tilde{V}_W \end{cases}. \tag{15}$$

Fig. 2 shows the above theoretical solutions for the sliding problem between a triangular probe and a 1D viscoelastic foundation. The black solid line shows the solution (i.e., the dimensionless master curve). The blue and red broken lines show the asymptotic solutions for the low- and high-speed regions, respectively. When the drive speed is high, we see the outlet peeling of the viscoelastic foundation from the probe surface (i.e., decrease in b) in (a) and (b) and the vertical lift of the probe (i.e., decrease in δ) in (b). The friction coefficient linearly increases for low speed and shows constant for high speed in (a) and (b).

2.2.2. *Parabolic Probe*

In this section, we show the theoretical solutions for the 1D sliding problem of the parabolic probe. First, under constant-δ conditions, the dimensionless drive speed is [16]:

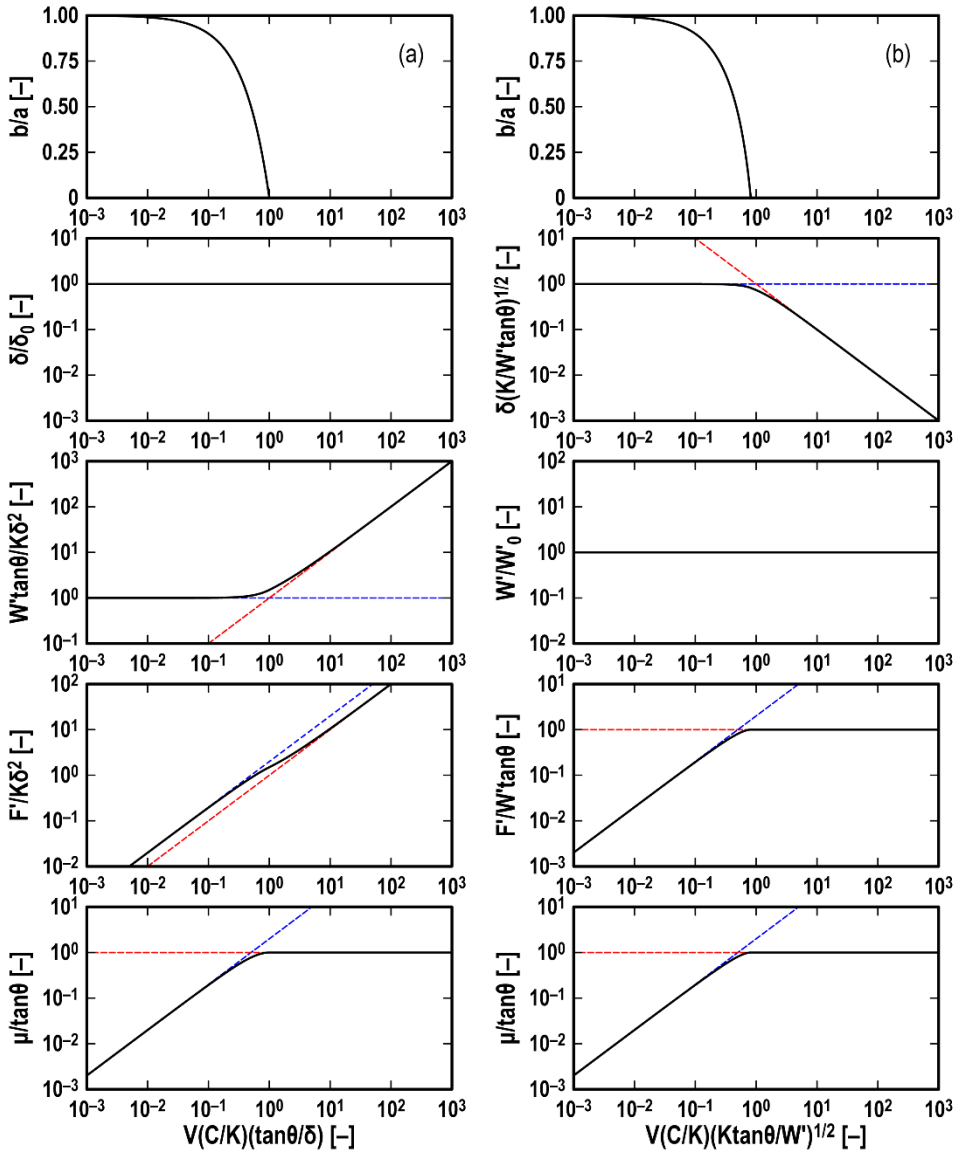

Fig. 2 Theoretical solutions for the sliding problem between a triangular probe and a 1D viscoelastic foundation under (a) constant-δ and (b) constant-W conditions.

$$\tilde{V}_\delta \equiv \frac{CV}{K\sqrt{2R\delta}}. \tag{16}$$

Then, the other dimensionless quantities under constant-δ conditions are given as the following explicit functions of the dimensionless drive speed [16]:

$$\beta \equiv \frac{b}{a} = -\tilde{V}_\delta + \sqrt{1+\tilde{V}_\delta^{\,2}}\,, \tag{17}$$

$$\tilde{W}_\delta \equiv \frac{W'}{K\sqrt{2R\delta^3}} = \frac{2}{3}\left(1-\tilde{V}_\delta^{\,3}+(1+\tilde{V}_\delta^{\,2})^{3/2}\right), \tag{18}$$

$$\tilde{F}_\delta \equiv \frac{F'}{K\delta^2} = \frac{2}{3}\left(2\tilde{V}_\delta - 3\tilde{V}_\delta^{\,2} - 2\tilde{V}_\delta^{\,4} + 2\tilde{V}_\delta(1+\tilde{V}_\delta^{\,2})^{3/2}\right), \tag{19}$$

$$\tilde{\mu}_\delta \equiv \mu\sqrt{\frac{2R}{\delta}} = \frac{2\tilde{V}_\delta - 3\tilde{V}_\delta^{\,2} - 2\tilde{V}_\delta^{\,4} + 2\tilde{V}_\delta(1+\tilde{V}_\delta^{\,2})^{3/2}}{1-\tilde{V}_\delta^{\,3}+(1+\tilde{V}_\delta^{\,2})^{3/2}}\,. \tag{20}$$

Then, under constant-W conditions, based on the relationship between δ and W' given by Equation (18), we obtain the following dimensionless drive speed [16]:

$$\tilde{V}_W = \left(\frac{2}{3}\right)^{-1/3} \tilde{V}_\delta \left(1-\tilde{V}_\delta^{\,3}+(1+\tilde{V}_\delta^{\,2})^{3/2}\right)^{-1/3}. \tag{21}$$

However, it is not easy to obtain the dimensionless drive speed for constant-δ conditions as an explicit function of that for constant-W conditions. In this case, it is reasonable to take the following implicit form [16]:

$$\tilde{V}_W \equiv \frac{CV}{K}\left(\frac{K}{2RW'}\right)^{1/3} = \tilde{V}_\delta \tilde{W}_\delta^{\,-1/3}. \tag{22}$$

This leads to the following implicit forms for the other dimensionless quantities [16]:

$$\beta \equiv \frac{b}{a} = -\tilde{V}_\delta + \sqrt{1+\tilde{V}_\delta^{\,2}}\,, \tag{23}$$

$$\tilde{\delta}_W \equiv \delta\left(\frac{32RK^2}{9W'^2}\right)^{1/3} = \left(\frac{4}{3}\right)^{2/3} \tilde{W}_\delta^{\,-2/3}, \tag{24}$$

$$\tilde{F}_W \equiv F'\left(\frac{4R^2K}{W'^4}\right)^{1/3} = \tilde{F}_\delta \tilde{W}_\delta^{\,-4/3}, \tag{25}$$

$$\tilde{\mu}_W \equiv \mu\left(\frac{4R^2K}{W'}\right)^{1/3} = \tilde{F}_\delta \tilde{W}_\delta^{\,-4/3}. \tag{26}$$

Fig. 3 shows the above theoretical solutions for the sliding problem between a parabolic probe and a 1D viscoelastic foundation. When the drive speed is high, we see the outlet peeling of the viscoelastic foundation in (a) and (b) and the vertical lift (i.e., decrease in δ) in (b). The friction coefficient linearly increases for low speed in (a) and (b). For high speed, it shows constant in (a) but decreases (b). The latter property, termed the velocity-weakening friction, is known for the source of stick-slip instabilities in sliding systems [25-32].

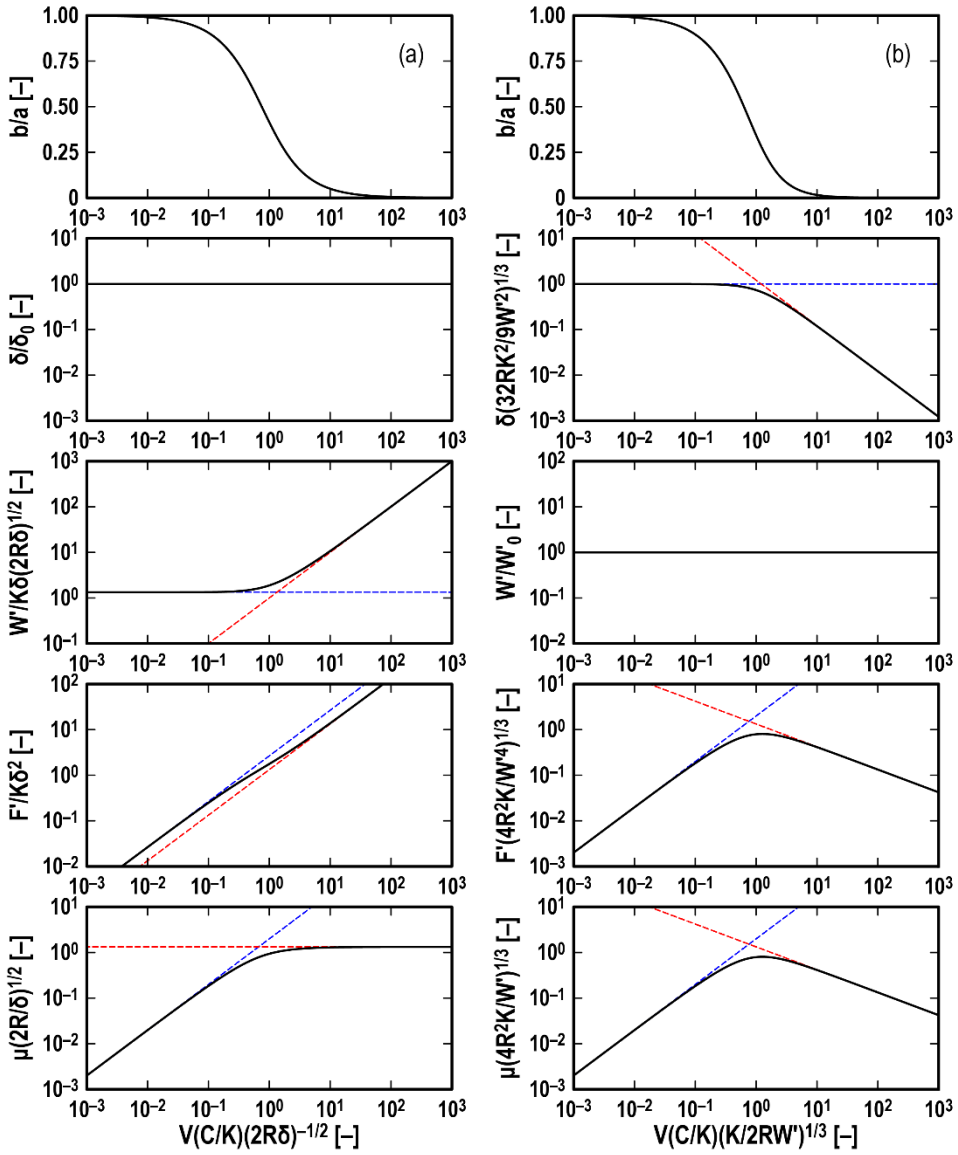

Fig. 3 Theoretical solutions for the sliding problem between a parabolic probe and a 1D viscoelastic foundation under (a) constant-δ and (b) constant-W conditions.

3. SLIDING CONTACTS OF RIGID PROBES WITH A 2D VISCOELASTIC FOUNDATION

3.1. Model for 2D Problems

In Section 3, we extend the 1D problems to consider the 2D problems for conical and paraboloidal probes:

$$h(x, y) = \tan\theta\sqrt{x^2 + y^2}\,, \tag{27}$$

$$h(x, y) = \frac{x^2 + y^2}{2R}\,. \tag{28}$$

The viscoelastic foundation is a 2D array of independent Kelvin-Voigt elements in the *xy*-plane, characterized by a stiffness (per unit area) K and a damping coefficient (per unit area) C. The normal load W and friction force F are:

$$W = \int_{-a(0)}^{a(0)} \int_{-a(y)}^{b(y)} \left(K\left(\delta - h\right) - CV\frac{\partial h}{\partial x} \right) \mathrm{d}x\mathrm{d}y\,, \tag{29}$$

$$F = \int_{-a(0)}^{a(0)} \int_{-a(y)}^{b(y)} -\frac{\partial h}{\partial x}\left(K\left(\delta - h\right) - CV\frac{\partial h}{\partial x} \right) \mathrm{d}x\mathrm{d}y\,. \tag{30}$$

The x-positions of leading and trailing edges are dependent on their y-position: $a = a(y)$ and $b = b(y)$, respectively. The former is determined geometrically, while the latter is determined dynamically (see Eq. (31)). The friction coefficient is obtained by $\mu = F/W$.

3.2. Theoretical Solutions for 2D Problems

3.2.1. *Conical probe*

In this section, we consider the 2D sliding problem of the conical probe. To determine the integral range of Eqs. (29) and (30), we must solve the following nonlinear equation:

$$\beta^4 - 2\tilde{V}_\delta\beta^3 + \left(2\frac{y^2}{a^2} + \tilde{V}_\delta^{\,2} - 1 \right)\beta^2 - 2\tilde{V}_\delta\frac{y^2}{a^2}\beta - \frac{y^2}{a^2} + \frac{y^4}{a^4} = 0\,, \tag{31}$$

where $a = a(0)$ and $\beta = \beta(y) = b(y)/a(0)$. This difficulty comes from the fact that the vertical section of a cone is (not triangular but) hyperbolic, except for the vertical section by the plane that intersects the cone tip. However, considering the limiting cases (i.e., low- and high-speed cases leading to $\beta = 1$ and 0, respectively) enables us to obtain asymptotic solutions. The asymptotic solutions for constant-δ conditions are:

$$\tilde{W}_\delta \equiv \frac{W\tan^2\theta}{K\delta^3} = \begin{cases} \dfrac{\pi}{3} & \text{for low speed} \\ \tilde{V}_\delta & \text{for high speed} \end{cases}\,, \tag{32}$$

$$\tilde{F}_\delta \equiv \frac{F\tan\theta}{K\delta^3} = \begin{cases} \dfrac{\pi}{2}\tilde{V}_\delta & \text{for low speed} \\ \dfrac{\pi}{4}\tilde{V}_\delta & \text{for high speed} \end{cases}, \tag{33}$$

$$\tilde{\mu}_\delta \equiv \frac{\mu}{\tan\theta} = \begin{cases} \dfrac{3}{2}\tilde{V}_\delta & \text{for low speed} \\ \dfrac{\pi}{4} & \text{for high speed} \end{cases}. \tag{34}$$

The asymptotic solutions for constant-W conditions are:

$$\tilde{\delta}_W \equiv \delta_W \left(\frac{3}{\pi}\frac{W\tan^2\theta}{K}\right)^{-1/3} = \begin{cases} 1 & \text{for low speed} \\ \left(\dfrac{\pi}{3}\right)^{1/3} \tilde{V}_W{}^{-1/2} & \text{for high speed} \end{cases}, \tag{35}$$

$$\tilde{F}_W \equiv \frac{F}{W\tan\theta} = \begin{cases} \left(\dfrac{9\pi}{8}\right)^{1/3} \tilde{V}_W & \text{for low speed} \\ \dfrac{\pi}{4} & \text{for high speed} \end{cases}, \tag{36}$$

$$\tilde{\mu}_W \equiv \frac{\mu}{\tan\theta} = \begin{cases} \left(\dfrac{9\pi}{8}\right)^{1/3} \tilde{V}_W & \text{for low speed} \\ \dfrac{\pi}{4} & \text{for high speed} \end{cases}. \tag{37}$$

Fig. 4 shows the theoretical solutions for the sliding problem between a conical probe and a 2D viscoelastic foundation, showing similar velocity dependences to those for the 1D problem of the triangular probe (see Fig. 2). A distinct difference can be seen in the velocity dependence of the indentation depth for high speed (i.e., δ is proportional to V^{-1} for the 1D problem and $V^{-1/2}$ for the 2D problem).

3.2.2. *Paraboloidal Probe*

In this section, we consider the 2D sliding problem of the paraboloidal probe. First, under constant-δ conditions, we can take the same dimensionless drive speed as that for the 1D problem of the parabolic probe (see Eq. (16)):

$$\tilde{V}_\delta \equiv \frac{CV}{K\sqrt{2R\delta}}. \tag{38}$$

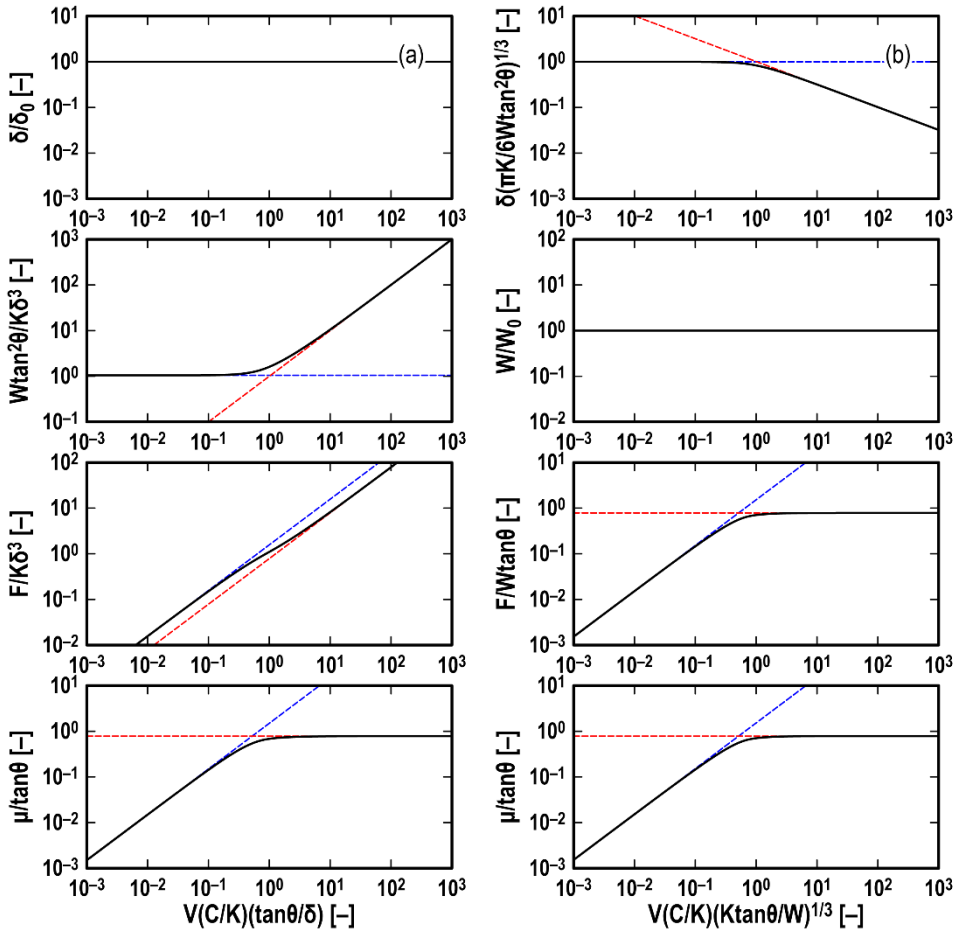

Fig. 4 Theoretical solutions for the sliding problem between a conical probe and a 2D viscoelastic foundation under (a) constant-δ and (b) constant-W conditions.

This simplicity comes from the fact that the vertical section of a paraboloid is always a parabola with an identical tip curvature radius. Then, we obtain the following explicit forms for the other dimensionless quantities under constant-δ conditions:

$$\tilde{W}_\delta \equiv \frac{W}{2KR\delta^2} = \frac{\pi}{4} + \frac{1}{2}\tilde{V}_\delta(1-\tilde{V}_\delta^{\,2}) + \frac{1}{2}(1+\tilde{V}_\delta^{\,2})^2 \arctan(\tilde{V}_\delta^{\,-1}) , \tag{39}$$

$$\tilde{F}_\delta \equiv \frac{F}{K\sqrt{2R\delta^5}} = \frac{\pi}{2}\tilde{V}_\delta - \frac{5}{3}\tilde{V}_\delta^{\,2} - \tilde{V}_\delta^{\,4} + \tilde{V}_\delta(1+\tilde{V}_\delta^{\,2})^2 \arctan(\tilde{V}_\delta^{\,-1}) , \tag{40}$$

$$\tilde{\mu}_\delta \equiv \mu\sqrt{\frac{2R}{\delta}} = \frac{3\pi + 6\tilde{V}_\delta(1-\tilde{V}_\delta^{\,2}) + 6(1+\tilde{V}_\delta^{\,2})^2 \arctan(\tilde{V}_\delta^{\,-1})}{6\pi\tilde{V}_\delta - 20\tilde{V}_\delta^{\,2} - 12\tilde{V}_\delta^{\,4} + 12\tilde{V}_\delta(1+\tilde{V}_\delta^{\,2})^2 \arctan(\tilde{V}_\delta^{\,-1})} . \tag{41}$$

Then, under constant-W conditions, based on the relationship between δ and W given by Eq. (39), we obtain the following dimensionless drive speed:

$$\tilde{V}_W = \tilde{V}_\delta \left(\frac{\pi}{4} + \frac{1}{2}\tilde{V}_\delta (1 - \tilde{V}_\delta^{\,2}) + \frac{1}{2}(1 + \tilde{V}_\delta^{\,2})^2 \arctan(\tilde{V}_\delta^{\,-1}) \right)^{-1/4}. \tag{42}$$

However, it is not easy to obtain the dimensionless drive speed for constant-δ conditions as an explicit function of that for constant-W conditions, as in the case for the 1D problem of the parabolic probe (see Section 2.2.2). In this case, it is reasonable to take the following implicit form:

$$\tilde{V}_W = \tilde{V}_\delta \tilde{W}_\delta^{\,-1/4} = \frac{CV}{K} \left(\frac{K}{2RW} \right)^{1/4}. \tag{43}$$

This leads to the following implicit forms for the other dimensionless quantities:

$$\tilde{\delta}_W \equiv \delta \left(\frac{\pi RK}{W} \right)^{1/2} = \left(\frac{\tilde{W}_\delta}{\tilde{W}_{\delta 0}} \right)^{-1/2}, \tag{44}$$

$$\tilde{F}_W \equiv F \left(\frac{8R^3K}{W^5} \right)^{1/4} = \tilde{F}_\delta \tilde{W}_\delta^{\,-5/4}, \tag{45}$$

$$\tilde{\mu}_W \equiv \mu \left(\frac{8R^3K}{W} \right)^{1/4} = \tilde{F}_\delta \tilde{W}_\delta^{\,-5/4}. \tag{46}$$

Fig. 5 shows the theoretical solutions for the sliding problem between a paraboloidal probe and a 2D viscoelastic foundation, showing similar velocity dependences to those for the 1D problem of the parabolic probe (see Fig. 3). Some distinct differences can be seen in the velocity dependences of the indentation depth, friction force, and friction coefficient for high speed (i.e., δ is proportional to V^{-1} for the 1D problem and $V^{-2/3}$ for the 2D problem; F and μ are proportional to $V^{-1/2}$ for the 1D problem and $V^{-1/3}$ for the 2D problem).

4. SLIDING CONTACTS OF RIGID PROBES WITH A 3D VISCOELASTIC HALF-SPACE

4.1. Basics of the Method of Dimensionality Reduction (MDR)

In Section 4, we consider 3D problems between an axisymmetric rigid probe having the shape $z = f(r)$ and a 3D viscoelastic half-space with the plane surface characterized by Kelvin-Voigt model with shear modulus G and dynamical viscosity η. As most elastomers have Poisson ratio close to 1/2, we assume that the medium is incompressible. Under these assumptions, the application of the MDR consists of the following two steps [18]:

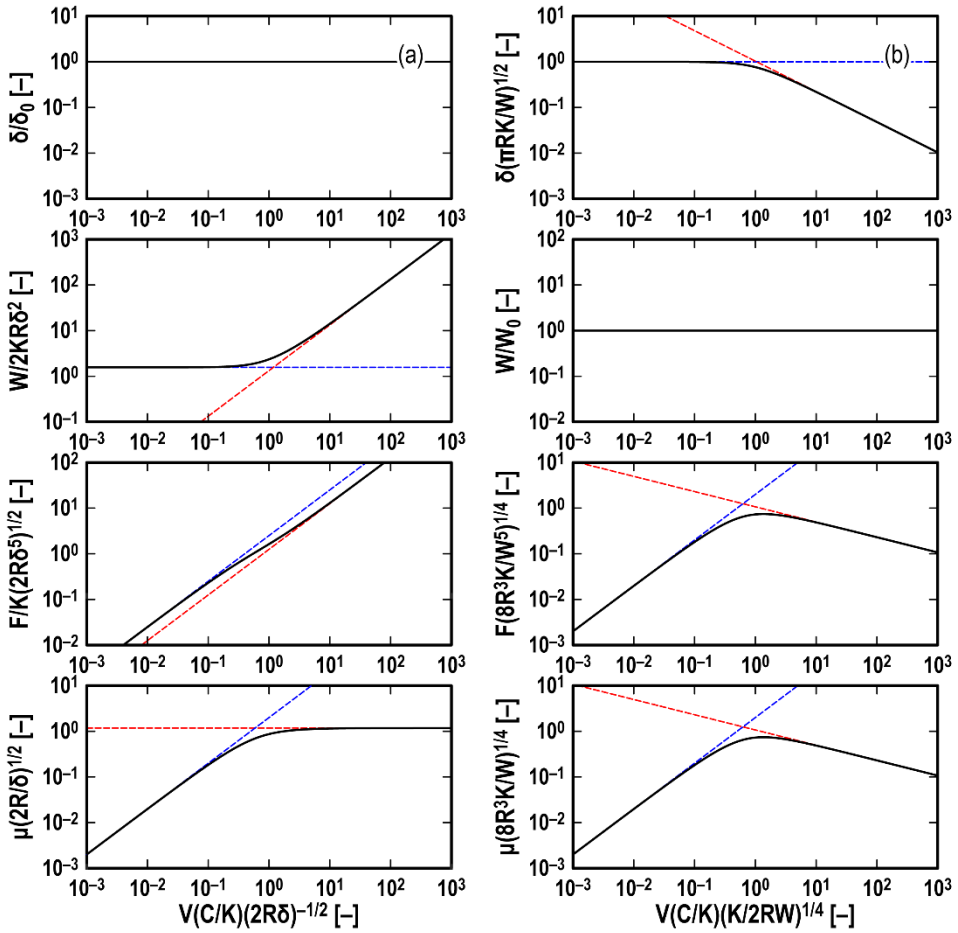

Fig. 5 Theoretical solutions for the sliding problem between a paraboloidal probe and a 2D viscoelastic foundation under (a) constant-δ and (b) constant-W conditions.

Step I: The 3D viscoelastic body is replaced by a 1D viscoelastic foundation consisting of an array of non-interacting Kelvin-Voigt elements which stiffness k and damping coefficient c are defined as follows:

$$k = 4G\Delta x\,,\ \ c = 4\eta\Delta x\,, \tag{47}$$

where Δx is spacing between adjacent elements.

Step II: The 3D profile $z = f(r)$ is transformed into a 1D profile $g(x)$ according to:

$$g(x) = |x| \int_0^{|x|} \frac{f'(r)}{\sqrt{x^2 - r^2}} \mathrm{d}r\,. \tag{48}$$

In particular, triangular and parabolic profiles are transformed as follows [18]:

$$f(r) = r\tan\theta_{3D} \Rightarrow g(x) = \frac{\pi}{2}|x|\tan\theta_{3D}, \tag{49}$$

$$f(r) = \frac{r^2}{2R_{3D}} \Rightarrow g(x) = \frac{x^2}{R_{3D}}. \tag{50}$$

Now the transformed shape $g(x)$ is pressed into the viscoelastic foundation by the depth δ and moved tangentially with a given velocity v. To obtain the results which apply to the initial 3D problem, the coefficients of friction obtained by the above MDR procedure should be multiplied with 0.67 for triangular probes and 0.55 for parabolic probes [23]. This means that the solutions obtained in Section 2 can be applied – after corresponding coordinate transformation – to contacts with the 3D half-space.

4.2. Theoretical Solutions for 3D Problems

4.2.1. *Conical Probe*

Comparison of shape and material parameter definitions given by Eqs. (1) and (3) with those of the MDR, Eqs. (49) and (47), shows that the following variable change must be undertaken:

$$\tan\theta \Rightarrow \frac{\pi}{2}\tan\theta_{3D},\ K \Rightarrow 4G,\ C \Rightarrow 4\eta,\ W' \Rightarrow W,\ F' \Rightarrow F. \tag{51}$$

For the main governing parameter, the dimensionless speed (5), we obtain:

$$\tilde{V}_\delta \equiv \frac{\pi\eta V\tan\theta_{3D}}{2G\delta}. \tag{52}$$

Applying variable transformation (51) to (9) and using the scaling coefficient 0.67 for conical probes [23] yields:

$$\mu \approx 1.05\tan\theta_{3D}\begin{cases}\dfrac{4\tilde{V}_\delta - \tilde{V}_\delta^{\,2}}{2+\tilde{V}_\delta^{\,2}} & \text{for}\quad 0 \le \tilde{V}_\delta \le 1\\ 1 & \text{for}\quad 1 \le \tilde{V}_\delta\end{cases}. \tag{53}$$

This equation provides the coefficient of friction of a 3D cone in contact with a Kelvin-Voigt half-space under conditions of fixed indentation depth.

The governing parameter for the case of a fixed normal force, Eq. (10), becomes

$$\tilde{V}_W \equiv \frac{\eta V}{G}\left(\frac{2\pi G\tan\theta_{3D}}{W}\right)^{1/2}, \tag{54}$$

and the coefficient of friction (15) becomes:

$$\mu = 1.05\tan\theta_{3D}\begin{cases}\tilde{V}_W\sqrt{4-2\tilde{V}_W^{\,2}} - \dfrac{1}{2}\tilde{V}_W^{\,2} & \text{for}\quad 0 \le \tilde{V}_W \le \sqrt{\dfrac{2}{3}}\\ 1 & \text{for}\quad \sqrt{\dfrac{2}{3}} \le \tilde{V}_W\end{cases}. \tag{55}$$

4.2.2. *Paraboloidal Probe*

Comparison of shape and material parameter definitions given by Eqs. (2) and (3) with those of the MDR, Eqs. (50) and (47), shows that the following variable change must be undertaken:

$$R \Rightarrow \frac{R_{3D}}{2}\,,\ K \Rightarrow 4G\,,\ C \Rightarrow 4\eta\,,\ W' \Rightarrow F_N\,,\ F' \Rightarrow F_x\,. \tag{56}$$

The dimensionless drive speed (16) becomes:

$$\tilde{V}_\delta \equiv \frac{\eta V}{G\sqrt{R_{3D}\delta}}\,. \tag{57}$$

Applying transformations (57) and scaling with factor 0.55 for the parabolic profile, we receive:

$$\mu = 0.55\sqrt{\frac{\delta}{R_{3D}}}\,\frac{2\tilde{V}_\delta - 3\tilde{V}_\delta^{\,2} - 2\tilde{V}_\delta^{\,4} + 2\tilde{V}_\delta(1+\tilde{V}_\delta^{\,2})^{3/2}}{1-\tilde{V}_\delta^{\,3} + (1+\tilde{V}_\delta^{\,2})^{3/2}}\,. \tag{58}$$

For the case of fixed force, the governing dimensionless drive speed (22) becomes:

$$\tilde{V}_W \equiv \frac{\eta V}{G}\left(\frac{4G}{R_{3D}W}\right)^{1/3}\,. \tag{59}$$

The scaling (26) of the coefficient of friction becomes:

$$\tilde{\mu}_W \equiv 0.55\mu\left(\frac{4R_{3D}^2 G}{W}\right)^{1/3}\,. \tag{60}$$

With definitions (59) and (60), the results reported above in Fig. 3 are applicable to the 3D case.

5. CONCLUSION

In this paper, we discussed 1D, 2D, and 3D sliding problems of typical rigid probes (triangular and parabolic probes in the 1D and conical and paraboloidal probes in the 2D and 3D) in contact with 1D and 2D viscoelastic foundations and a viscoelastic half-space, respectively. We found that extending the 1D to the 2D models does not change the master curves qualitatively, confirming that the simplest 1D model is a remarkable tool for understanding sliding friction due to solid viscoelasticity. Applying the MDR to the 1D model is expected to estimate the sliding friction more quantitatively.

Acknowledgement: *This study was supported by CREST (Grant Number JPMJCR2193) of the Japan Science and Technology Agency (JST), KAKENHI (Grant Number 21H01236) of the Japan Society for the Promotion of Science (JSPS), and by Deutsche Forschungsgemeinschaft (Grant Number 423918021).*

REFERENCES

1. Moore D.F., Geyer W., 1974, *A review of hysteresis theories for elastomers*, Wear, 30(1), pp. 1-34.
2. Papangelo, A., Ciavarella, M., 2022, *Viscoelastic dissipation in repeated normal indentation of an Hertzian profile*, International Journal of Solid and Structures, 236-237, 111362.
3. Popov, V.L., 2017, *Contact Mechanics and Friction: Physical Principles and Applications*, Springer Berlin, 391 p.
4. Wineman, A.S., Rajagopal, K.R., 2000, *Mechanical Response of Polymers. An Introduction*, Cambridge University Press, 317 p.
5. Forstenhäusler, M., López-Guerra, E.A., Solares, S.D., 2021, *Guidelines to simulate viscoelastic materials with an arbitrary number of characteristic times in the context of atomic force microscopy*, Facta Universitatis, Series: Mechanical Engineering, 19(1), pp. 133-153.
6. Hunter, S.C., 1961, *The rolling contact of a rigid cylinder with a viscoelastic half space*, Journal of Applied Mechanics, 28(4), pp. 611-617.
7. Menga, N., Putignano, C., Carbone, G., Demelio, G.P., 2014, *The sliding contact of a rigid wavy surface with a viscoelastic half-space*, Proceedings of the Royal Society A, 470, 20140392.
8. Ciavarella, M., Papangelo, A., 2019, *Some simple results on the multiscale viscoelastic friction*, Facta Universitatis Series Mechanical Engineering, 17(2), pp. 191-205.
9. Carbone, G., Mandriota, C., Menga, N., 2022, *Theory of viscoelastic adhesion and friction*, Extreme Mechanics Letters, 56, 101877.
10. Johnson, K.L., 1985, *Contact Mechanics*, Cambridge University Press.
11. May, W.D., Morris, E.L., Atack, D., 1959, *Rolling friction of a hard cylinder over a viscoelastic material*, Journal of Applied Physics, 30(11), pp. 1713-1724.
12. Flom, D.G., Bueche, A.M., 1959, *Theory of rolling friction for spheres*, Journal of Applied Physics, 30(11), pp. 1725-1730.
13. Pöschel, T., Schwager, T., Brilliantov, N.V., 1999, *Rolling friction of a hard cylinder on a viscous plane*, European Physical Journal B: Condensed Matter and Complex Systems, 10, pp. 169-174.
14. Martinez-Martinez, D., van der Pal, J.P., Pei, Y.T., De Hosson, J.Th.M., 2011, *Performance of diamond-like carbon-protected rubber under cyclic friction. II. Influence of substrate viscoelasticity on the friction evolution*, Journal of Applied Physics, 110, 124907.
15. Nakano, K., Kono, M., 2020, *Transient and steady sliding friction of elastomers: Impact of vertical lift*, Frontiers in Mechanical Engineering, 6, 38.
16. Watanabe, T., Hatanaka, S., Nakano, K., 2023, *Dimensionless numbers and master curves for sliding friction from the Kelvin-Voigt viscoelasticity of solids*, Tribology Online, 18(6), pp. 406-416.
17. Watanabe, T., Nakano, K., 2024, *Two origins for bell-shaped velocity-dependent friction coefficient: Kelvin-Voigt or standard linear solid viscoelasticity*, Tribology Online, 19(3), pp. 167-177.
18. Popov, V.L., Heß, M., Willert, E., 2019, *Handbook of Contact Mechanics. Exact Solutions of Axisymmetric Contact Problems*, Springer Berlin.
19. Grosch, K.A., 1963, *The relation between the friction and visco-elastic properties of rubber*, Proceedings of the Royal Society A, 274(1356), pp. 21-39.
20. Heinrich, G., 1997, *Hysteresis friction of sliding rubbers on rough and fractal surfaces*, Rubber Chemistry and Technology, 70(1), pp. 1-14.
21. Persson, B.N.J., 1998, *On the theory of rubber friction*, Surface Science, 401(3), pp. 445-454.
22. Persson, B.N.J., Tosatti, E., 2000, *Qualitative theory of rubber friction and wear*, The Journal of Chemical Physics, 112(4), pp. 2021-2029.
23. Kürschner, S., 2014, *Friction between a rigid body and a model elastomer having a linear viscous rheology*, ZAMM - Journal of Applied Mathematics and Mechanics / Zeitschrift Für Angewandte Mathematik und Mechanik, 95(8), pp. 822-830.
24. Kusche, S., 2016, *Frictional force between a rotationally symmetric indenter and a viscoelastic half-space*, ZAMM - Journal of Applied Mathematics and Mechanics / Zeitschrift Für Angewandte Mathematik Und Mechanik, 97(2), pp.226-239.
25. Persson, B.N.J., 2000, *Sliding Friction: Physical Principles and Applications*, Springer-Verlag Berlin.
26. Thompson, D.J., Jones, C.J.C., 2000, *A review of the modelling of wheel/rail noise generation*, Journal of Sound and Vibration, 231(3), pp. 519-536.
27. Nakano, K., 2006, *Two dimensionless parameters controlling the occurrence of stick-slip motion in a 1-DOF system with Coulomb friction*, Tribology Letters, 24(2), pp. 91-98.
28. Kado, N., Tadokoro, C., Nakano, K., 2014, *Kinetic friction coefficient measured in tribotesting: Influence of frictional vibration*, Tribology Online, 9(2), pp. 63-70.

29. Kim, J.W., Joo, B.S., Jang, H., 2019, *The effect of contact area on velocity weakening of the friction coefficient and friction instability: A case study on brake friction materials*, Tribology International, 135, pp. 38-45.
30. Nakano, K., Popov, V.L., 2020, *Dynamic stiction without static friction: The role of friction vector rotation*, Physical Review E, 102(6), 063001.
31. Papangelo, A., Putignano, C., Hoffmann, N., 2020, *Self-excited vibrations due to viscoelastic interactions*, Mechanical Systems and Signal Processing, 144, 106894.
32. Pal, A., Restrepo, V., Goswami, D., Martinez, R.V., 2021, *Exploiting mechanical instabilities in soft robotics: Control, sensing, and actuation*, Advanced Materials, 33(19), 2006939.